Maternal microbiota *Bifidobacterium* promotes placental vascularization, nutrient transport and fetal growth in mice

Authors: Jorge Lopez-Tello[1]*, Zoe Schofield[2]*, Raymond Kiu[2], Matthew J. Dalby[2], Douwe van Sinderen[3], Gwénaëlle Le Gall[4], Amanda N Sferruzzi-Perri[1†], Lindsay J Hall[2,5†]

Affiliations:

[1]Department of Physiology, Development, and Neuroscience, Centre for Trophoblast Research, University of Cambridge, Cambridge, UK

[2]Gut Microbes & Health, Quadram Institute Bioscience, Norwich Research Park, Norwich, UK

[3]APC Microbiome Institute, University College Cork, Cork, Ireland

[4]Norwich Medical School, University of East Anglia, Bob Champion Research and Education Building, James Watson Road, Norwich Research Park, Norwich NR4 7UQ, UK

[5]Chair of Intestinal Microbiome, School of Life Sciences, ZIEL – Institute for Food & Health, Technical University of Munich, Freising, Germany

[*†]Contributed equally

Corresponding author names: Jorge Lopez-Tello (jl898@cam.ac.uk), Amanda N. Sferruzzi-Perrri (ans48@cam.ac.uk) &Lindsay Hall (lindsay.hall@tum.de **I** Lindsay.Hall@quadram.ac.uk)

Author Contributions: JL-T, ZS, ANS-P, LJH designed research; JL-T, ZS, RK, GLG conducted research, JL-T, ZS, RK, MJD contributed analytic tools and performed analysis; DvS contributed reagents; JL-T, ZS, ANS-P, LJH wrote the paper with feedback from all the authors.

Competing Interest Statement: The authors declare that they have no competing interests.

Classification: Biological Sciences – Physiology

Keywords: Pregnancy, Placenta, Microbiota, Fetus, *Bifidobacterium*

This file includes:

Main Text: 5,638

Main Figures: 3

Tables: 1

Supplementary Figures: 3

Supplementary Tables: 3

References: 46

Significance: Metabolism is highly influenced by the gut microbiota, which is particularly important during gestation, when key metabolites are used for feto-placental growth. However, the contribution of the maternal gut microbiota (and its microbiota-generated metabolites) in determining fetal outcomes is largely unexplored. Here, we show that maternal gut communities and specific microbiota members are key modulators of placental phenotype with important consequences for fetal development. We have revealed novel roles for a maternal *Bifidobacterium* species, that include the control of placental capillary morphogenesis and nutrient transporters (glucose and lipids), which affect fetal metabolism and growth. Our work has important implications for the establishment of novel therapeutic strategies to treat pregnancy complications.

Abstract

The gut microbiota plays a central role in regulating host metabolism. However, while substantial progress has been made in discerning how the microbiota influences host functions post birth and beyond, little has been carried out into understanding how key members of the maternal gut microbiota can influence feto-placental growth. Here, using germ-free and specific-pathogen-free mice, we demonstrate that the bacterium *Bifidobacterium breve* UCC2003 modulates maternal body adaptations, placental vasculature growth and nutrient transporter capacity, with implications for fetal metabolism and growth. The effects of *B. breve* UCC2003 on feto-placental growth are mediated, in part, by changes in the maternal and

placental metabolome (*i.e.* acetate and carnitine). Analysis of placental vascular bed confirmed that *Bifidobacterium* improves fetal capillary elongation via changes in *Igf2P0, Dlk1* and *Mapk14* expression. Additionally, *B. breve* UCC2003, acting through *Slc2a1* and *Fatp3-4* transporters, was shown to restore fetal glycaemia and improve fetal growth in association with changes in the fetal hepatic transcriptome. This study provides knowledge towards a novel and safe therapeutic strategy for treating pregnancy disorders via modulation of the maternal gut microbiota.

Main Text

Introduction

All nutrients and metabolites required for feto-placental growth are provided by the mother, which in turn is thought to be influenced by the maternal gut microbiota through breakdown of complex dietary components (1). During gestation, liberated metabolites may be used by the placenta for morphogenesis, and transported across the placenta for use by the fetus for growth and development (2, 3). This is highly important in late gestation, when fetal growth is maximal, and aligns with alterations in the maternal microbiota, including increasingly higher levels of the beneficial bacterial genus *Bifidobacterium* (4–6). Failure of the mother to provide nutrients and metabolites to the fetus can result in pregnancy complications including small for gestational age (SGA), fetal loss and stillbirth. However, the contribution of the maternal microbiota in determining fetal outcomes is largely unexplored, although knowledge in this area would be highly valuable for developing treatments to improve fetal growth, with benefits for population health.

Here, we hypothesized that the maternal gut microbiota, and specific microbiota members, regulate fetal growth by modulating placental development and nutrient supply. We tested this hypothesis by comparing conceptus growth in three different maternal gut microbiota conditions by using germ-free (GF) mice, conventional specific-pathogen-free (SPF) mice and maternal GF mice colonized with *Bifidobacterium breve* UCC2003 (7). As a keystone microbiota member and ‘probiotic’ species, *B. breve* may represent a suitable option for

treating pregnancy complications by exerting beneficial metabolic effects on maternal physiology and associated feto-placental growth. Indeed, *B. breve* induced changes in maternal physiology, placental morphogenesis and the abundance of placental glucose and lipid transporters, which were associated with improvements in growth and metabolism of the fetus.

Results

Germ-free mice treated with B. breve have altered body composition and caecum metabolic profile

To assess whether maternal microbiota is able to influence feto-placental growth, GF mice were treated orally with *B. breve* UCC2003 from day 10 of gestation (treatment on days 10, 12 and 14; i.e. BIF group), and compared to GF and SPF dams (for experimental overview see Figure S1, and *B. breve* colonization levels Figure S2).

Maternal body composition differed between groups with GF and BIF mice showing increased digestive tract weight and lower pancreas mass compared to SPF mice. GF and BIF mice had similar circulating concentrations of glucose and insulin to SPF mice (assessed in fed conditions; Table 1). Compared to SPF mice, treatment with *B. breve* reduced maternal gonadal fat depot, liver, and spleen weights in BIF mice. No differences were observed in the circulating concentrations of leptin, cholesterol, triglycerides, or free fatty acids in maternal serum (Table 1).

Metabolomics analysis in maternal caecum samples indicated that the concentration of 13 out of 115 metabolites were significantly altered (Table 1 and Table S1). Acetate was significantly influenced by *B. breve* (Table 1), with BIF dams having intermediate concentrations compared to SPF and GF mice (the low levels of acetate detectable in GF mice, most likely originated from the diet and/or are host-derived). These findings suggest that acetate producing *B. breve* and the wider gut microbiota may exert selective effects on maternal metabolic and immune organs.

Maternal gut microbiota and B. breve regulate fetal growth by controlling fetal glycaemia

Although the three experimental groups had similar numbers of viable fetuses per litter, the GF group had higher rates of resorptions (fetal losses) compared to SPF and BIF mice (Figure 1A-B). In fact, all GF dams had at least one resorption, whilst BIF reduced the appearance of resorptions by 50%. Conceptus mass (defined as the sum of fetal weight and its placenta) and fetal growth were significantly impaired in GF mice by the lack of the maternal microbiota, whilst these two parameters were improved with the administration of *B. breve* (Figure 1C-D). Compared to SPF and BIF mice, GF fetuses were smaller, with reduced liver weight, but preserved brain size. Fetuses from GF mice also displayed hypoglycaemia compared to SPF and BIF groups (Figure 1D-G). *B. breve* improved fetal weight and restored fetal glycaemia and liver growth. The rate of SGA, defined as fetuses below the 10^{th} percentile (≤495mg; SPF control population), was reduced in BIF compared to GF mice (Figure 1E). These findings highlight that the maternal microbiota, and *B. breve,* positively modulate fetal growth and metabolism.

Maternal B. breve modulates fetal hepatic transcriptome

The liver is a key organ for glucose storage and production. As fetuses from BIF mice had enlarged livers and improved glycaemia, we next determined if there were changes in the fetal hepatic transcriptome (data obtained on GD18.5, when fetal liver function is particularly active prior to term; Figure 1H). A total of 602 genes were differentially expressed, with 94 significantly up-regulated and 508 down-regulated genes in BIF group, when compared to GF group (Figure 1I-J). Functional enrichment analysis indicated many metabolic pathways were regulated in the fetal livers of BIF mice including carboxylic acid and lipid metabolic processes, steroid hydroxylase activity, fatty acid metabolism and response to glucocorticoid (Figure 1K; Supplementary Table 1). Therefore, maternal *B. breve* appear to exert beneficial alterations in fetal hepatic function to support fetal growth.

Maternal gut microbiota and B. breve control placental morphogenesis

To further understand the links between the maternal microbiota and the regulation of fetal growth, we assessed placental structure. When compared to SPF mice, placentas were lighter in GF and BIF mice without changes in placental efficiency (Figure 2A-B). Analysis of placental compartments showed that lack of maternal gut microbiota significantly hampered growth of the placental labyrinth transport zone (Lz), without compromising the endocrine junctional zone or decidua volumes (Figure 2C). It also did not affect placental glycogen storage (Figure 2D). Structural analysis of the Lz showed that although the volume of the trophoblast was unaffected, maternal blood spaces were reduced in both GF and BIF mice compared to SPF (Figure 2E-F). Moreover, in the GF group, the volume of fetal capillaries and surface area for exchange of the Lz were shown to be reduced; effects that were partially ameliorated in BIF mice (Figure 2G-H). The barrier between maternal and fetal blood was also determined to be thinner in BIF *versus* GF mice (Figure 2F-I). Lz apoptosis levels were similar between groups (Figure 2J).

To define the molecular mechanisms behind the expansion of the Lz, and increased fetal capillary volume in the BIF mice, we quantified the expression of select genes in micro-dissected Lz. Common angiogenic factors *Vegf, Ang1, Ang2* were similarly expressed between groups (Figure 2K). However, the expression of signaling pathways involved in cell proliferation and growth, namely the MAPK pathway, was significantly altered by changes in maternal gut microbiota; *Mapk1* was shown to be increased in both GF and BIF, while *Mapk14* (also known as *p38Mapk*) was revealed to be specifically up-regulated in the Lz of BIF mice. In addition, *Dlk1* and *Igf2P0*, which are key genes implicated in metabolism and Lz formation, were significantly up-regulated in the BIF group (Figure 2K). The expression of *Akt* did not vary with group. Overall, these findings suggest that the maternal gut microbiota, and *B. breve,* regulate the development of the mouse placental Lz via modulation of specific cell growth and metabolic genes.

Maternal gut microbiota and B. breve do not affect placental glucocorticoid handling, but controls key placental nutrient transporters

Glucocorticoids are a class of steroid hormones that can affect both fetal and placental formation. To control glucocorticoid actions on the conceptus, the placenta expresses 11β-hydroxysteroid dehydrogenase type 1 and 2 (*11Hsd1* and *11Hsd2*). We found that the expression of these genes was unaltered in the Lz by changes in the maternal gut microbiota (no changes between SPF, GF or BIF; Figure 2L). To better understand the changes in fetal growth and glycemia between groups, we quantified the expression of selected amino acid, glucose and lipid transporters in the Lz. We found no difference in the expression of system A amino acid transporters (*Slc38a1, Slc38a2, Slc38a4*) between groups (Figure 2M). However, the key glucose transporter *Slc2a1* was up-regulated in the Lz of BIF mice compared to GF mice, with intermediate values for SPF (*Slc2a3* mRNA levels were similar between groups; Figure 2N). Expression of specific fatty acid transporters (*Fatp3* and *Fatp4*) was also increased in BIF compared to GF mice (with intermediate values for SPF and no change in *Cd36, Fatp1* or *Fatp6* between groups; Figure 2N). Collectively, these data suggest that maternal gut microbiota, and *B. breve*, regulate fetal growth by inducing changes in the expression of key nutrient transporters within the placenta.

Differences in placental labyrinth growth are linked to an altered placental metabolome

To gain further mechanistic understanding of the changes observed in the placental Lz and fetal liver, we analysed >80 metabolites at GD16.5 (Figure 3 and Table S1). We found 5 metabolites significantly altered in the placental Lz (Figure 3). Aminoadipic acid in the Lz was very low in GF/BIF groups as well as in fetal livers (Figure 3A). Treatment with *B. breve* significantly reduced the concentrations of acetylcarnitine and carnitine in Lz tissue compared to SPF placentas, but not in fetal livers (Figure 3B-C). Levels of formate in placental Lz were significantly elevated in both GF and BIF compared to SPF mice (Figure 3D), with a similar trend (although not significant) in fetal liver samples. Acetate was also altered in the Lz (Figure 3E), with concentrations significantly lower in the SPF compared to the GF group, whilst BIF samples showed intermediate levels (although these levels were much lower than observed in the maternal caecum). Similar to formate, concentrations of acetate in fetal liver followed

similar directions to the Lz, yet were not statistically different between groups. These data suggest that maternal gut microbiota, and *B. breve*, regulate the fetal and placental growth via modulation of the placental Lz metabolome.

Discussion

In this study, we provide evidence that the maternal microbiota and *B. breve* regulate maternal body composition during gestation and beneficially modulate feto-placental growth. To the best of our knowledge, this is the first demonstration of a maternal gut bacterium remotely controlling placental vascular growth and nutrient transporters, with important implications for fetal glycaemia and fetal growth. We observed that the effects of *Bifidobacterium* are partially mediated by altered metabolites in maternal caecum and in placental Lz tissue, with alterations in the expression of key genes in the placental Lz and fetal liver.

Bifidobacterium is the dominant microbiota member in vaginally delivered, breast fed infants, with certain species and strains known to stimulate and aid the maturation of the immune system (8). *B. breve* UCC2003 also regulates responses at the gut barrier, inducing homeostatic epithelial cell programming, and protecting against inflammatory insults (9, 10). Importantly, pregnancy is accompanied by increasing *Bifidobacterium* abundance in the gut of women and mice (5), which is associated with changes in progesterone concentrations during pregnancy. Additionally, alterations in the abundance of *Bifidobacterium* are also linked to the development of serious pregnancy complications like preeclampsia (11). Our study shows that *B. breve* improves pregnancy outcomes in mice, as indicated by lower numbers of resorptions and an increased number of normally grown fetuses within the litter (5). *B. breve* UCC2003 was also shown to induce changes in the metabolite milieu, including acetate, acetylcarnitine and carnitine in the mother and placenta, which were likely key for the beneficial effects on fetal growth. Acetate is a major bifidobacterial fermentation by-product, which directly mediates epithelial cell responses but also exerts systemic beneficial metabolic effects (12, 13). More generally, microbial-derived short-chain fatty acids (SCFAs) modulate multiple host physiological systems and during pregnancy are associated with maternal gestational weight, neonatal length and body weight, and protection against allergic airway disease in the

developing fetus (14, 15). Acetate crosses the placenta (15), so in our model, the elevated maternal *B. breve*-derived acetate may exert beneficial effects on feto-placental growth via (i) maternal effects, through interactions within the maternal gut mucosa as evidenced by higher maternal caecum acetate concentrations in *B. breve* supplemented (and SPF) dams vs. GF and the subsequent impact on maternal organs (liver, adipose and spleen) and nutrient handling, (ii) effects on the placenta, through use of acetate for cellular metabolism, growth and function, and/or (iii) effects on the fetal metabolism following transport of acetate across the placenta to the fetus. Compared to the maternal caecum, levels of acetate were relatively low in the placental Lz and fetal liver (for all 3 groups). This suggests that *B. breve* (and SPF microbiota)-derived acetate may be used to support anabolic processes *in utero* (hence the very low levels detected), and together with changes in acetylcarnitine and carnitine, may be supported by our observations of elevated fatty acid transporter expression in the placenta and differentially regulated genes in the fetal liver. The observed modulation of immune-associated pathways in the fetal liver, including those associated with G protein-coupled receptor signalling (e.g. *Dusp9*), also indicates a role for direct acetate-associated responses (16). Moreover, previous work in adult mice suggests elevation of gut acetate levels due to *Bifidobacterium* treatment plays a key role in regulating glucose handling systemically, and reduces visceral fat accumulation (linking to our observation of reduced maternal gonadal fat deposition in *B. breve*-treated dams) (17). *B. breve* supplementation also restored fetal glycaemia in GF mice, achieving similar values to that seen for SPF fetuses. Previous *in vivo* studies indicate different strains of *Bifidobacterium* (including *B. breve*) modulate glucose handling (18), with this genus also consistently associated with potential protection against human metabolic disorders e.g. type 2 diabetes (19, 20).

B. breve was shown to significantly improve the placental vascular bed by modifying the elongation of their fetal capillary network, which is required for adequate fetal growth (21). The mechanisms governing this improvement could be partially mediated by changes in the expression of two imprinted genes (22), *Igf2* (namely the placenta-exclusive isoform, *Igf2P0*) and *Dlk1*, and via MAPK upregulation (specifically *Mapk14*). In this regard, deletion of *Igf2P0* results in feto-placental growth restriction in association with reduced placental surface area

for exchange, fetal capillary volume and increased barrier thickness (reviewed by (23)); parameters that were all improved by *B breve* UCC2003 in line with the *Igf2P0* mRNA upregulation). Interestingly, *Igf2P0* is important for the structural and transport adaptations occurring in the placenta in response to maternal nutritional restriction (24). *Dlk1,* a non-canonical ligand of the Notch signalling pathway localized to the endothelial cells of fetal capillaries in the placental Lz, also regulates placental vascularisation and branching morphogenesis (25). In addition, IGF2 and DLK1 can both mediate cellular actions via the MAPK pathway (26, 27). *Mapk14*, also known as p38MAPK, forms part of a signal transduction pathway that has been linked to environmental stresses and inflammatory cytokines (28). However, p38MAPK also regulates many normal cellular processes, including proliferation and cytoskeletal organisation. Furthermore, research in mice has demonstrated that *Mapk14* is essential for embryogenesis and placental Lz angiogenesis and vascular remodeling (29). In addition, placentas exposed to *B. breve* UCC2003, had lower concentrations of acetylcarnitine and carnitine compared to SPF, suggesting a greater reliance on these compounds for energy production, or enhanced transfer of these fatty acids to the fetus (30). Carnitine is well-known for mediating the transport of fatty acids into mitochondrial matrix for fatty acid β-oxidation. Carnitine can also promote p38MAPK signalling activation in cardiac tissue (31). Taken together, placental structural, transport and metabolic changes seen with *B. breve* UCC2003 treatment may link to the altered metabolites/nutrient milieu in the mother and would have been beneficial in providing additional substrates for fetal growth and development (when compared to GF; Supplementary Figure 3).

While our study has clear strengths and strong translational implications for pregnancy complication treatments, it also has certain limitations. Unsurprisingly, we did not see a full 'rescue' of all placental and fetal responses in the monocolonised GF *B. breve* (BIF) group, compared to complex microbiota found in SPF dams. An array of gut-associated signaling and a diverse metabolite pool are expected to provide more complete fetal development and programming. Indeed, other or additional *Bifidobacterium* species and/or strains may be required for placental and fetal development, given strain-specific host physiology responses (10, 32). Further studies should allow the relative contributions of other microbial- and

Bifidobacterium-derived factors to be elucidated. Nonetheless, this study has revealed novel roles for *Bifidobacterium* and provides a safe therapeutic strategy for treating pregnancy complications, suggesting an opportunity for *in utero* programming through maternal *Bifidobacterium* and associated metabolites.

Overall, our study highlights the importance of the maternal gut microbiota during gestation and demonstrates that *B. breve* modulates maternal physiology, placental capillarization and nutrient transporter capacity with impact on fetal glycaemia and fetal growth. Our findings prompt an in-depth investigation into how additional members of the gut microbiota impact on pregnancy outcomes. These future studies are important for the design of novel therapies to combat fetal growth restriction and other pregnancy complications.

Materials and Methods

***Bifidobacterium breve* UCC2003/pCheMC**

B. breve UCC2003/pCheMC was generated by introducing the plasmid pCheMC to electrocompetent *B. breve* UCC2003 as described previously (33). In brief, *B. breve* UCC2003 was grown until mid-log phase, chilled on ice and washed twice with ice cold sucrose citrate buffer (1mM citrate, 0.5M sucrose, pH5.8) and then electroporation of cells was carried out under the following conditions; 25 MF, 200 Ohms, 2 KV. Transformed cells were incubated for 2 hours in Reinforced Clostridial Medium (RCM) at 37ºC in a controlled anaerobic chamber then plated (34) on RCM agar plates with selective antibiotics. Colonies were sub-cultured 3 times on RCM agar plates with selective antibiotics. Antibiotics were used at the following final concentrations erythromycin 2µg/mL.

Lyophilised *B breve*

B. breve was grown in De Man, Rogosa and Sharpe agar (MRS) under anaerobic conditions overnight. The bacterial cell pellet was resuspended in 10% milk powder and lyophilised in 200 ml quantities. Lyophilised *B. breve* was reconstituted with 500µl PBS. Concentration of *B. breve* was 10^{10}CFU/ml. All batches were tested for contamination upon reconstitution on Luria-

Bertani (LB) and Brain-Heart Infusion (BHI) plates under anaerobic and aerobic conditions at 37°C. No contamination of *B. breve* was detected.

Mice

All mouse experiments were performed under the UK Regulation of Animals (Scientific Procedures) Act of 1986. The project license PDADA1B0C under which these studies were carried out was approved by the UK Home Office and the UEA Ethical Review Committee. All mice were housed in the Disease Modelling Unit at the University of East Anglia, UK. Animals were housed in a 12:12 hour light/dark, temperature-controlled room and allowed food and water ad libitum. Female Germ Free C57BL/6J (GF) and Specific Pathogen Free (SPF) mice aged 6-8 weeks were used for the study. GF mice were bred in germ free isolators (2 females to 1 male) and on gestational day (GD) GD9.5, pregnant mice (confirmed by weight) were removed from the GF isolator and transferred to individually ventilated cages. The sterility of these cages was previously tested and found to be suitable for housing GF mice for 1 week. Sterile water was changed every 2 days. At GD10, mice were dosed by oral gavage with 100µL of *B. breve* UCC2003 at 10^{10} CFU/mL or 100µL vehicle control (PBS, 4 % skimmed milk powder). At GD16.5 and GD18.5, mice were sacrificed by cervical dislocation and samples collected for molecular and histological analysis. The experimental design can be found in Supplementary Figure 1.

B. breve colonisation levels

Faecal samples were checked for contamination and *B. breve* colonisation. Briefly, faecal samples from GF and GF treated with *B. breve* were diluted in 500 µL of PBS and agitated for 30 mins at 4˚C on an Eppendorf MixMate 5353 Digital Mixer Plate Shaker. The faecal solution was passed through a 0.45µm syringe filter. Faecal solution was diluted 1 in 100 and 20 µL was added to a De Man, Rogosa and Sharpe agar plate with erythromycin and incubated for 48 hours in an anaerobic chamber at 37˚C. Colony forming units were counted using a click counter.

Blood hormones and circulating metabolites

Maternal blood was obtained by cardiac exsanguination immediately after cervical dislocation. Blood was centrifuged and serum collected and stored at -80ºC until further analysis. Blood glucose and plasma concentrations of leptin, insulin, triglycerides, cholesterol, and free fatty acids were determined as previously reported (35). Fetal blood glucose levels were measured with a handheld glucometer (One Touch Ultra; LifeScan) immediately after decapitation of the fetus.

Placental histology

Placentas were cut in half and fixed in 4% paraformaldehyde overnight at 4ºC. Samples were washed 3 times with PBS for 15 minutes each and storage in 70% ethanol until embedding in wax. Embedded placentas were cut at 5µm thickness and stained with haematoxylin and eosin for gross morphology. Placental layer volumes were calculated using the Computer Assisted Stereological Toolbox (CAST v2.0). For analysis of labyrinth components, sections were stained with lectin for identification of fetal endothelial vessels and with cytokeratin for trophoblasts. Further details of the double-labelling immunohistochemistry and the analysis performed can be found elsewhere (36). For the analysis of placental glycogen, sections were stained with Periodic acid–Schiff (Sigma-Aldrich) previous incubation with 0.5% periodic acid (Thermo Fisher Scientific). Sections were counterstained with Fast-green (Sigma-Aldrich) and digitalized with the nanozoomer scanner (Hamamatsu). Analysis of placental glycogen accumulation was performed with Image J and conducted blinded to experimental groups. TUNEL staining for placental cell death was performed using the TUNEL Assay Kit - HRP-DAB (Abcam, ab206386) following manufacturer instructions except for the counterstaining which was substituted for Nuclear Fast Red (Vector). Sections were digitalized using a nanozoomer scanner (Hamamatsu) and the amount of apoptosis in the labyrinth zone was calculated in 5 random areas (x20 magnification) and analysed by Image J software.

RNA extraction and qPCR

Extraction of RNA from micro-dissected placental labyrinth zones was performed with RNeasy Plus Mini Kit (Qiagen) and reverse transcribed using the High Capacity cDNA RT Kit minus RT

inhibitor (Applied Biosystems) according to manufacturer's instructions. Samples were analysed using MESA Blue SYBR (Eurogentec) and primers (See Supplementary Table 3) were synthesized by Sigma-Aldrich. The expression of each gene was normalized to the geometric mean expression of two reference genes *Hprt* and *Ubc*, which remained stably expressed across the groups. Analysis was performed using the 2-ΔΔCt method (37).

Sequence pre-processing, Differential Gene Expression (DGE) analysis and Functional enrichment analysis

Fetal liver RNA on GD18.5 was extracted using the RNeasy Plus Mini Kit (Qiagen). RNA sequence pre-processing and DGE analysis was performed as previously described with slight modifications (9). Briefly, FASTQ reads were initially quality-filtered using fastp v0.20.0 with options -q 10 (sequence reads with phred quality <10 were discarded). Subsequently, sequence reads for each sample were merged (merge-paired-reads.sh) and followed by rRNA sequence filtering via SortMeRNA v2.1 based on SILVA rRNA database optimised for SortMeRNA software (38, 39). Filtered reads were then unmerged (unmerge-paired-reads.sh) and ready for transcript quantification. Transcript mapping and quantification were then performed using Kallisto v0.44.0 (40). *Mus musculus* (C57BL/6 mouse) cDNA sequences (GRCm38.release-98_k31) retrieved from Ensembl database were indexed with Kallisto utility *index* at default parameter and was used for following transcript mapping and abundance quantification via Kallisto utility *quant* at 100 bootstrap replicates (-b 100) (41).

RNA raw counts were subjected (Kallisto outputs) to DGE analysis, which was performed using R library *Sleuth* (v0.30.0) (42). Transcripts were then mapped to individual genes using Ensembl BioMart database (GRCm38.p6) with function *sleuth_prep* and option *gene_mode = TRUE*. Genes with an absolute $\log_2$ (fold change) >1.0 and q value <0.05 (p-adjusted value; based on Wald test statistics) were considered to be differentially regulated (43). DGE statistics were plotted via functions within package *Sleuth*. Finally, functional enrichment analysis was performed using g:Profiler webtool g:GOst based on organism *Mus Musculus* species (44). Briefly, a list of DGEs (Ensembl IDs) was uploaded to g:GOst, then selected 'GO

molecular function', 'GO biological process' and 'Reactome' in the 'data sources'. Significance threshold was set at 0.001 (g:SCS threshold).

Metabolite extraction, Nuclear Magnetic Resonance (NMR) spectroscopy and metabolite quantification

Extraction of metabolite from liver, placenta, caecum contents and culture (spent) media samples were performed as previously described as a standard protocol (45). For caecal samples, frozen materials (stored at -80°C prior to analysis) were weighed ~50 mg before the addition of 600 µL of faecal water phosphate buffer solution. The faecal water phosphate buffer was prepared as follows: add 0.51g $NaH_2PO_4.H_2O$ and 2.82g K_2HPO_4 to 200 mL D_2O (Deuterium Oxide; Merck). To this, 34.5 mg TSP (Trimethylsilyl propanoic acid; used as NMR standard) and 100 mg NaN_3 (Merck) were added (46). Next, the mixture was centrifuged for 10 min at 17,000 x g before transferring the mixture to an NMR tube (Merck) for subsequent NMR analysis.

For liver and placenta samples (stored at -80°C prior to analysis), frozen fresh tissue (~20-45 mg) was placed into a 2 ml sterile microcentrifuge tube pre-loaded with ~15-20 glass beads (Merck) while 200 µL of ice-cold methanol (Fisher Scientific) and 42.5 µL of ultra-pure cold water were added to it and vortexed. Tissue was disrupted via a tissue lyser (Qiagen) for 2 x 2 mins. 100 µL of ice-cold chloroform (Merck) was then added and vortexed. 100 µL of ice-cold chloroform and 100 µL of ultra-pure cold water were added to the mixture, and kept on ice for 15 min. Liquid was then transferred into a new sterile microcentrifuge tube and centrifuged for 3 min at 17,000 x g. The top aqueous phase was transferred into a new microcentrifuge tube and speed-vacuumed for 30 min at 50°C and 30 min without heating prior to reconstitution with faecal water phosphate buffer solution at 600 µL. The mixture was then moved to an NMR tube (Merck) for subsequent NMR analysis. Metabolites from culture media Brain Heart Infusion (BHI; Oxoid) and spent media (BHI cultured with *B. breve* UCC2003 for 48 h) were extracted as follows: 400 µL of medium was transferred into a sterile microcentrifuge tube with the addition of 200 µL faecal phosphate buffer and mixed well. The mixture was then moved to an NMR tube (Merck) for further NMR analysis.

Samples in NMR tubes were subsequently subjected to NMR spectroscopy. The ^{1}H NMR spectra were recorded at 600 MHz on a Bruker AVANCE spectrometer (Bruker BioSpin GmbH, Germany) running Topspin 2.0 software. The metabolites were then quantified using the software Chenomx® NMR Suite 7.0™.

Statistical analysis

All statistical analysis and sample size are shown in each figure/table and in the corresponding figure/table legends. No statistical analysis was used to pre-determine sample size and samples were assigned code numbers and analysis was performed in a blinded fashion. Statistical calculations were performed using the GraphPad Prism software (GraphPad, San Diego, CA), and RStudio Version 1.4.1106 (RStudio Boston, MA) with R Version 4.0.3 (Vienna, Austria). Morphometric parameters of mother, placenta and fetus were analysed by one-way ANOVA followed by Tukey post hoc test. Differences between individual metabolites between the three groups were tested with a Kruskal-Wallis test using the kruskal.test function with correction for multiple comparisons applied using the Benjamini & Hochberg false discovery rate method using the p.adjust function. Pairwise comparisons between the three groups were carried out with a Dunn's test on individual metabolites significantly different after correction for multiple comparisons using the dunnTest function in the FSA package. SGA rate was analysed by contingency retrospective analysis and Fisher's exact test. ROUT test was used for identification of outlier values. A probability value of < 0.05 was considered significantly different.

Acknowledgments

JL-T currently holds a Sir Henry Wellcome Postdoctoral Fellowship (220456/Z/20/Z) and previously a Newton International Fellowship from the Royal Society (NF170988 / RG90199*)*. LJH is supported by Wellcome Trust Investigator Awards (100974/C/13/Z and 220876/Z/20/Z); the Biotechnology and Biological Sciences Research Council (BBSRC), Institute Strategic Programme Gut Microbes and Health (BB/R012490/1), and its constituent projects

BBS/E/F/000PR10353 and BBS/E/F/000PR10356. ANS-P is supported by a Lister Institute of Preventative Medicine Research Prize (RG93692).

Data availability

The fetal liver RNA-Seq raw sequencing data are deposited at the National Center for Biotechnology Information (NCBI) under BioProject PRJNA748000. Relevant data are within the manuscript and its Supporting Information files. Scripts for differential gene expression analysis can be accessed at GitHub, https://github.com/raymondkiu/Maternal-foetal-microbiota-paper/

Figure legends

Figure 1. Effects of maternal gut microbiome and *B. breve* supplementation during pregnancy on fetal viability, growth and hepatic transcriptome. (A) Number of viable fetuses per litter, **(B)** Number of resorptions per litter (left) and number of dams with presence of resorptions within the litter (right), **(C)** Conceptus mass defined as the sum of the fetus and placenta, **(D)** Fetal weight, **(E)** Rate of small for gestational age (SGA) defined as fetuses below the 10^{th} percentile (≤490mg), **(F)** Fetal organ weights, and **(G)** Fetal blood glucose concentrations on GD16.5, **(H-K)** RNA-Seq analysis of fetal liver samples obtained at GD18.5 (n=5/group), **(H)** PCA plot and **(I)** volcano plots showing up and down-regulated DEGs in BIF group (compared to GF group), **(J)** Heat map of the 20 most up and down-regulated DEGs (BIF group), **(K)** Functional profiling (g:Profiler) on 602 DEGs. Key enriched GO terms and REACTOME pathways are shown in the figure (significant threshold: $P_{adj}<0.001$). Statistical analysis for data shown in **A-G** was performed with ROUT test for outlier identification followed by one-way ANOVA Tukey multiple comparisons test. Data in **E** was analysed using contingency retrospectively analysis (Fisher's exact test). RNA-Seq data analysis is described in the material and methods section. Different superscripts indicate significant differences between groups (a *versus* b and/or c: $P<0.05$; mean±SEM). In figure **E**, *denotes differences compared to the SPF group and $^{\gamma}$symbol denotes differences between GF and BIF.

Figure 2. Effects of maternal gut microbiome and *B. breve* supplementation during pregnancy on placental structure and placental gene expression on GD16.5. (A) Placenta weight, **(B)** Placental efficiency determined by dividing fetal by placental mass, **(C)** Placental regional analysis, **(D)** Representative staining of placental glycogen with PAS and glycogen abundance, **(E)** Representative image of lectin and cytokeratin staining for labyrinth zone structural quantification, **(F-I)** Stereological parameters determined in placental labyrinth zone, **(J)** Representative image of TUNEL staining for apoptosis quantification in labyrinth zone **(K-O),** Gene expression levels in micro-dissected labyrinth zones (n=13/11/14 for SPF, GF and BIF respectively). ROUT test was used for identification of outlier values. Data were analyzed by one-way ANOVA followed by Tukey multiple comparisons test. Different superscripts indicate significant differences between groups (a *versus* b: P<0.05; mean±SEM).

Figure 3. Metabolomic profiling of placental labyrinth zone and fetal liver on GD16.5. Data were analysed by Kruskal-Wallis test followed by multiple comparisons using the Benjamini & Hochberg false discovery rate method and Dunn's test. ROUT test was used for identification of outlier values. Different superscripts indicate significant differences between groups (a *versus* b, P<0.05). Data presented as mean±SEM.

Supplementary Figure 1. Schematic representation of the experimental design.
B. breve was administrated by oral gavage on gestational day (GD) 10, 12 and 14 to germ-free mice. Abbreviations: LZ (placental labyrinth zone); SPF (Specific-Pathogen-Free mouse); GF (Germ-Free mouse); BIF (Germ-Free mouse treated with *B. breve* UCC2003).

Supplementary Figure 2. Colonization levels of *B. breve* determined in maternal faecal samples. Analysis performed by student-t test (****P<0.0001). Data displayed as mean ± SEM. Number of dams for GF (white bar) and BIF (grey bar) are 5 and 6, respectively.

Supplementary Figure 3. Summary illustration showing how the maternal gut bacteria and *B. breve* affects mother, placenta and fetus during gestation. Abbreviations: LZ (placental labyrinth zone); SPF (Specific-Pathogen-Free mouse); GF (Germ-Free mouse); BIF

(Germ-Free mouse treated with *B. breve* UCC2003); MBS (Maternal Blood Spaces); FC (Fetal Capillaries); SA (Surface Area); SGA (Small Gestational Age)

Table 1. Effects of maternal gut microbiome and *B. breve* administration during pregnancy on maternal body composition, circulating metabolites and hormones in maternal serum, and metabolites in caecum. Body composition and metabolites/hormones in serum were analyzed by one-way ANOVA followed by Tukey multiple comparisons test. Metabolites in maternal caecum were analysed by Kruskal-Wallis test followed by multiple comparisons using the Benjamini & Hochberg false discovery rate method and Dunn's test. ROUT test was used for identification of outlier values. Different superscripts indicate significant differences between groups (a *versus* b, P<0.05) (*P<0.05; **P<0.01; ***P<0.001; ****P<0.0001; NS: not significant). Data presented as mean±SEM.

Supplementary Table 1. List of differentially expressed genes and pathways detected in the liver RNA-Seq

Supplementary Table 2. List of metabolites analysed in maternal caecum, placental labyrinth zone and fetal liver on day 16 of gestation.

Supplementary Table 3. List of primers used for placental labyrinth zone qPCR

References

1. R. Krajmalnik-Brown, Z.-E. Ilhan, D.-W. Kang, J. K. DiBaise, Effects of Gut Microbes on Nutrient Absorption and Energy Regulation. *Nutr Clin Pract* **27**, 201–214 (2012).
2. B. McDonald, K. D. McCoy, Maternal microbiota in pregnancy and early life. *Science* **365**, 984–985 (2019).
3. M. G. de Agüero, *et al.*, The maternal microbiota drives early postnatal innate immune development. *Science* **351**, 1296–1302 (2016).
4. O. Koren, *et al.*, Host remodeling of the gut microbiome and metabolic changes during pregnancy. *Cell* **150**, 470–480 (2012).
5. M. Nuriel-Ohayon, *et al.*, Progesterone Increases Bifidobacterium Relative Abundance during Late Pregnancy. *Cell Rep* **27**, 730-736.e3 (2019).

6. T. Napso, H. Yong, J. Lopez-Tello, A. N. Sferruzzi-Perri, The role of placental hormones in mediating maternal adaptations to support pregnancy and lactation. *Front. Physiol.* **9** (2018).
7. K. Pokusaeva, G. F. Fitzgerald, D. van Sinderen, Carbohydrate metabolism in Bifidobacteria. *Genes Nutr* **6**, 285–306 (2011).
8. M. J. Dalby, L. J. Hall, Recent advances in understanding the neonatal microbiome. *F1000Res* **9**, F1000 Faculty Rev-422 (2020).
9. R. Kiu, *et al.*, Bifidobacterium breve UCC2003 Induces a Distinct Global Transcriptomic Program in Neonatal Murine Intestinal Epithelial Cells. *iScience* **23**, 101336 (2020).
10. K. R. Hughes, *et al.*, Bifidobacterium breve reduces apoptotic epithelial cell shedding in an exopolysaccharide and MyD88-dependent manner. *Open Biol* **7**, 160155 (2017).
11. T. Miao, *et al.*, Decrease in abundance of bacteria of the genus Bifidobacterium in gut microbiota may be related to pre-eclampsia progression in women from East China. *Food & Nutrition Research* (2021) https:/doi.org/10.29219/fnr.v65.5781 (July 5, 2021).
12. S. Fukuda, *et al.*, Bifidobacteria can protect from enteropathogenic infection through production of acetate. *Nature* **469**, 543–547 (2011).
13. M. A. González Hernández, E. E. Canfora, J. W. E. Jocken, E. E. Blaak, The Short-Chain Fatty Acid Acetate in Body Weight Control and Insulin Sensitivity. *Nutrients* **11**, 1943 (2019).
14. M. Priyadarshini, *et al.*, Maternal short-chain fatty acids are associated with metabolic parameters in mothers and newborns. *Transl Res* **164**, 153–157 (2014).
15. A. N. Thorburn, *et al.*, Evidence that asthma is a developmental origin disease influenced by maternal diet and bacterial metabolites. *Nat Commun* **6**, 7320 (2015).
16. C. H. Kim, Control of lymphocyte functions by gut microbiota-derived short-chain fatty acids. *Cell Mol Immunol* **18**, 1161–1171 (2021).
17. R. Aoki, *et al.*, A proliferative probiotic Bifidobacterium strain in the gut ameliorates progression of metabolic disorders via microbiota modulation and acetate elevation. *Sci Rep* **7**, 43522 (2017).
18. K. Kikuchi, M. Ben Othman, K. Sakamoto, Sterilized bifidobacteria suppressed fat accumulation and blood glucose level. *Biochem Biophys Res Commun* **501**, 1041–1047 (2018).
19. H. Wu, *et al.*, Metformin alters the gut microbiome of individuals with treatment-naive type 2 diabetes, contributing to the therapeutic effects of the drug. *Nat Med* **23**, 850–858 (2017).
20. A. Solito, *et al.*, Supplementation with Bifidobacterium breve BR03 and B632 strains improved insulin sensitivity in children and adolescents with obesity in a cross-over, randomized double-blind placebo-controlled trial. *Clinical Nutrition* **40**, 4585–4594 (2021).
21. J. López-Tello, *et al.*, Fetal and trophoblast PI3K p110α have distinct roles in regulating resource supply to the growing fetus in mice. *Elife* **8** (2019).
22. J. M. Frost, G. E. Moore, The Importance of Imprinting in the Human Placenta. *PLOS Genetics* **6**, e1001015 (2010).
23. A. N. Sferruzzi-Perri, I. Sandovici, M. Constancia, A. L. Fowden, Placental phenotype and the insulin-like growth factors: resource allocation to fetal growth. *J Physiol* **595**, 5057–5093 (2017).

24. A. N. Sferruzzi-Perri, *et al.*, Placental-specific Igf2 deficiency alters developmental adaptations to undernutrition in mice. *Endocrinology* **152**, 3202–3212 (2011).
25. A. Yevtodiyenko, J. V. Schmidt, Dlk1 expression marks developing endothelium and sites of branching morphogenesis in the mouse embryo and placenta. *Developmental Dynamics* **235**, 1115–1123 (2006).
26. C.-C. Huang, *et al.*, Soluble delta-like 1 homolog (DLK1) stimulates angiogenesis through Notch1/Akt/eNOS signaling in endothelial cells. *Angiogenesis* **21**, 299–312 (2018).
27. K. Forbes, M. Westwood, P. N. Baker, J. D. Aplin, Insulin-like growth factor I and II regulate the life cycle of trophoblast in the developing human placenta. *American Journal of Physiology-Cell Physiology* **294**, C1313–C1322 (2008).
28. A. Cuenda, S. Rousseau, p38 MAP-Kinases pathway regulation, function and role in human diseases. *Biochimica et Biophysica Acta (BBA) - Molecular Cell Research* **1773**, 1358–1375 (2007).
29. J. S. Mudgett, *et al.*, Essential role for p38α mitogen-activated protein kinase in placental angiogenesis. *PNAS* **97**, 10454–10459 (2000).
30. A. N. Sferruzzi-Perri, J. S. Higgins, O. R. Vaughan, A. J. Murray, A. L. Fowden, Placental mitochondria adapt developmentally and in response to hypoxia to support fetal growth. *Proc. Natl. Acad. Sci. U.S.A.* **116**, 1621–1626 (2019).
31. Z. Fan, Y. Han, Y. Ye, C. Liu, H. Cai, l-carnitine preserves cardiac function by activating p38 MAPK/Nrf2 signalling in hearts exposed to irradiation. *European Journal of Pharmacology* **804**, 7–12 (2017).
32. L. Ruiz, S. Delgado, P. Ruas-Madiedo, B. Sánchez, A. Margolles, Bifidobacteria and Their Molecular Communication with the Immune System. *Front Microbiol* **8**, 2345 (2017).
33. A. Mazé, M. O'Connell-Motherway, G. F. Fitzgerald, J. Deutscher, D. van Sinderen, Identification and Characterization of a Fructose Phosphotransferase System in Bifidobacterium breve UCC2003. *Applied and Environmental Microbiology* **73**, 545 (2007).
34. M. Cronin, *et al.*, High Resolution In Vivo Bioluminescent Imaging for the Study of Bacterial Tumour Targeting. *PLOS ONE* **7**, e30940 (2012).
35. B. Musial, *et al.*, Proximity to Delivery Alters Insulin Sensitivity and Glucose Metabolism in Pregnant Mice. *Diabetes* **65**, 851–860 (2016).
36. K. De Clercq, J. Lopez-Tello, J. Vriens, A. N. Sferruzzi-Perri, Double-label immunohistochemistry to assess labyrinth structure of the mouse placenta with stereology. *Placenta* **94**, 44–47 (2020).
37. K. J. Livak, T. D. Schmittgen, Analysis of relative gene expression data using real-time quantitative PCR and the 2(-Delta Delta C(T)) Method. *Methods* **25**, 402–408 (2001).
38. S. Chen, Y. Zhou, Y. Chen, J. Gu, fastp: an ultra-fast all-in-one FASTQ preprocessor. *Bioinformatics* **34**, i884–i890 (2018).
39. E. Kopylova, L. Noé, H. Touzet, SortMeRNA: fast and accurate filtering of ribosomal RNAs in metatranscriptomic data. *Bioinformatics* **28**, 3211–3217 (2012).
40. N. L. Bray, H. Pimentel, P. Melsted, L. Pachter, Near-optimal probabilistic RNA-seq quantification. *Nat Biotechnol* **34**, 525–527 (2016).
41. D. R. Zerbino, *et al.*, Ensembl 2018. *Nucleic Acids Res* **46**, D754–D761 (2018).
42. H. Pimentel, N. L. Bray, S. Puente, P. Melsted, L. Pachter, Differential analysis of RNA-seq incorporating quantification uncertainty. *Nat Methods* **14**, 687–690 (2017).

43. R. J. Kinsella, *et al.*, Ensembl BioMarts: a hub for data retrieval across taxonomic space. *Database (Oxford)* **2011**, bar030 (2011).
44. U. Raudvere, *et al.*, g:Profiler: a web server for functional enrichment analysis and conversions of gene lists (2019 update). *Nucleic Acids Res* **47**, W191–W198 (2019).
45. G. Le Gall, Sample collection and preparation of biofluids and extracts for NMR spectroscopy. *Methods Mol Biol* **1277**, 15–28 (2015).
46. J. Wu, Y. An, J. Yao, Y. Wang, H. Tang, An optimised sample preparation method for NMR-based faecal metabonomic analysis. *Analyst* **135**, 1023–1030 (2010).

687 Table 1

688

689

690

691

Body composition				
	SPF (n=6)	GF (n=5)	BIF (n=6)	
Hysterectomy weight (g)	26.01±0.91	27.87±0.78	27.17±0.80	NS
Digestive Tract (g)	2.76±0.03^{a}	6.83±0.32^{b}	7.25±0.63^{b}	****
Caecum (g)	0.66±0.03^{a}	3.47±0.25^{b}	3.96±0.41^{b}	****
Small intestine (g)	1.66±0.03^{a}	2.65±0.11^{b}	2.59±0.14^{b}	****
Pancreas (mg)	315.40±30.12^{a}	183.40±24.74^{b}	190.60±38.71^{b}	*
Gonadal fat (mg)	433.10±43.20^{a}	297.0±37.02^{ab}	272.0±27.35^{b}	*
Liver (g)	2.09±0.10^{a}	1.79±0.05^{ab}	1.55±0.08^{b}	**
Spleen (mg)	117.90±2.80^{a}	91.76±10.60^{ab}	83.03±6.72^{b}	*
Circulating metabolites and metabolic hormones				
	SPF (n=6)	GF (n=5)	BIF (n=6)	
Glucose (mmol/L)	8.08±0.78	8.38±1.18	8.88±0.74	NS
Insulin (µg/L)	0.12±0.004	0.19±0.05	0.20±0.06	NS
Leptin (pg/mL)	2465±177.1	2739±486	2425±303	NS
Cholesterol (mmol/L)	1.33±0.03	1.56±0.08	1.41±0.09	NS
Triglycerides (mmol/L)	1.54±0.08	1.79±0.14	1.50±0.11	NS
Free Fatty Acids (µmol/L)	890.6±101.3	1440±362	1092±114.5	NS
Caecum Metabolites				
	SPF (n=3)	GF (n=4)	BIF (n=4)	
2.Methylbutyrate (mmol/Kg)	0.05±0.01^{a}	0±0.0^{b}	0±0.0^{b}	*
Isobutyrate (mmol/Kg)	0.41±0.24^{a}	0±0.0^{b}	0±0.0^{b}	*
Butyrate (mmol/Kg)	12.48±7.97^{a}	0±0.0^{b}	0±0.0^{b}	*
5.Aminopentanoate (mmol/Kg)	0.33±0.14^{a}	0±0.0^{b}	0±0.0^{b}	*
Propionate (mmol/Kg)	4.48±1.99^{a}	0±0.0^{b}	0±0.0^{b}	*
Citrulline (mmol/Kg)	0.30±0.07^{a}	0±0.0^{b}	0±0.0^{b}	*
Fucose (mmol/Kg)	0.08±0.02^{a}	0±0.0^{b}	0±0.0^{b}	*
Trimethylamine (mmol/Kg)	0.06±0.006^{a}	0±0.0^{b}	0±0.0^{b}	*
Isovalerate (mmol/Kg)	0.09±0.01^{a}	0±0.0^{b}	0±0.0^{b}	*
Methylamine (mmol/Kg)	0.05±0.02^{a}	0±0.0^{b}	0±0.0^{b}	*
Malonate (mmol/Kg)	0.09±0.02^{a}	0±0.0^{b}	0±0.0^{b}	*
Valerate (mmol/Kg)	0.57±0.27^{a}	0±0.0^{b}	0±0.0^{b}	*
Acetate (mmol/Kg)	35.49±20.66^{a}	0.55±0.06^{b}	3.79±1.64^{ab}	*

692 Supplementary Table 1 (Excel)

693 Supplementary Table 2 (Excel)

694 Supplementary Table 3

	Forward	*Reverse*
Hprt	*CAGGCCAGACTTTGTTGGAT*	*TTGCGCTCATCTTAGGCTTT*
Ubc	*GGAGTCGCCCGAGGTCA*	*AAAGATCTGCATCGTCTCTCTCAC*
Vegf	*GAAGCTACTGCCGTCCGATT*	*CTTCATCGTTACAGCAGCC*
Ang1	*GAAGCAACTTCTCAACAGACA*	*TTCTTTGTGTTTTCCCTCCATT*
Ang2	*CTTCTACCTCGCTGGTGAAGAG*	*GCTAAAATCACTTCCTGGTTGG*
Akt	*GCCGCCTGATCAAGTTCTCC*	*TTCAGATGATCCATGCGGGG*
Mapk1	*TGCTTTCTCTCCCGCACAAA*	*GGCCAGAGCCTGTTCAACTT*
Mapk14	*AGCTGTCGAGACCGTTTCAG*	*GATGGGTCACCAGGTACACG*
Dlk1	*GAAAGGACTGCCAGCACAAG*	*CACAGAAGTTGCCTGAGAAGC*
Igf2P0	*GAGGAAGCTCTGCTGTTTGG*	*CAAAGAGATGAGAAGCACCAAC*
Hsd11b1	*GAGGAAGGTCTCCAGAAGGTA*	*ATGTCCAGTCCGCCCAT*
Hsd11b2	*GGCTGGATCGCGTTGTC*	*CGTGAAGCCCATGGCAT*
Slc38a1	*CGGCGCCTTTCCCTTTATTTC*	*CCGTTAACTCGAGGCCACTT*
Slc38a2	*TTCTGATTGTGGTGATTTGCAAGAA*	*CAGGATGGGCACAGCATACA*
Slc38a4	*AAGGTAGAGGCGGGAAAGGG*	*AGGAACTTCTGACTTTCGGCA*
Slc2a1	*GCTTATGGGCTTCTCCAAACT*	*GGTGACACCTCTCCCACATAC*
Slc2a3	*GA TCGGCTCTTTCCAGTTTG*	*CAA TCA TGCCACCAACAGAG*
Cd36	*ATGGGCTGTGATCGGAACTG*	*GTCTTCCCAATAAGCATGTCTCC*
Fatp1	*GGCTCCTGGAGCAGGAACA*	*ACGGAAGTCCCAGAAACCAA*
Fatp3	*GAGAACTTGCCACCGTATGC*	*GGCCCCTATATCTTGGTCCA*
Fatp4	*GATTCTCCCTGTTGCTCCTGT*	*CCATTGAAGCAAACAGCAGG*
Fatp6	*AACCAAGTGGTGACATCTCTGC*	*TCCATAAAGTAAAGCGGGTCAG*

695

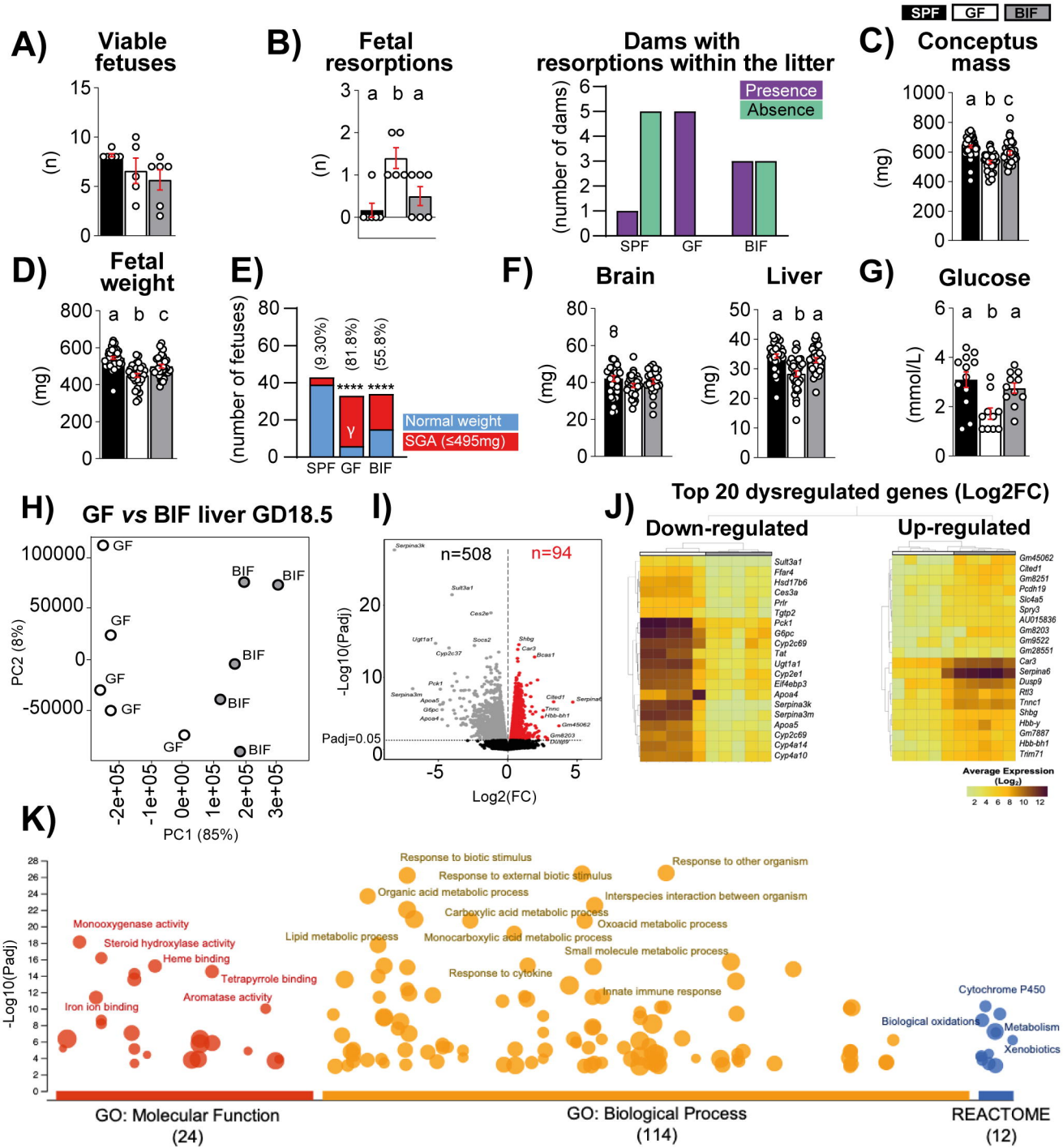
SPF
GF
BIF
A)
Viable fetuses
(n)
B)
Fetal resorptions
a b a
(n)
Dams with resorptions within the litter
(number of dams)
Presence
Absence
SPF
GF
BIF
C)
Conceptus mass
a b c
(mg)
D)
Fetal weight
a b c
(mg)
E)
(number of fetuses)
(9.30%)
(81.8%)
(55.8%)
****
****
γ
Normal weight
SGA (≤495mg)
SPF GF BIF
F)
Brain
a
(mg)
Liver
a b a
(mg)
G)
Glucose
a b a
(mmol/L)
H)
GF vs BIF liver GD18.5
PC2 (8%)
PC1 (85%)
I)
n=508
n=94
-Log10(Padj)
Padj=0.05
Log2(FC)
J)
Top 20 dysregulated genes (Log2FC)
Down-regulated
Up-regulated
Sult3a1
Ffar4
Hsd17b6
Ces3a
Prlr
Tgfp2
Pck1
G6pc
Cyp2c69
Tat
Ugt1a1
Cyp2e1
Eif4ebp3
Apoa4
Serpina3k
Serpina3m
Apoa5
Cyp2c69
Cyp4a14
Cyp4a10
Gm45062
Cited1
Gm8251
Pcdh19
Slc4a5
Spry3
AU015836
Gm8203
Gm9522
Gm28551
Car3
Serpina6
Dusp9
Rtl3
Tmnc1
Shbg
Hbb-y
Gm7887
Hbb-bh1
Trim71
Average Expression (Log2)
K)
-Log10(Padj)
Response to biotic stimulus
Response to other organism
Response to external biotic stimulus
Organic acid metabolic process
Interspecies interaction between organism
Carboxylic acid metabolic process
Oxoacid metabolic process
Monooxygenase activity
Steroid hydroxylase activity
Lipid metabolic process
Monocarboxylic acid metabolic process
Small molecule metabolic process
Heme binding
Tetrapyrrole binding
Response to cytokine
Aromatase activity
Innate immune response
Iron ion binding
Cytochrome P450
Biological oxidations
Metabolism
Xenobiotics
GO: Molecular Function
(24)
GO: Biological Process
(114)
REACTOME
(12)

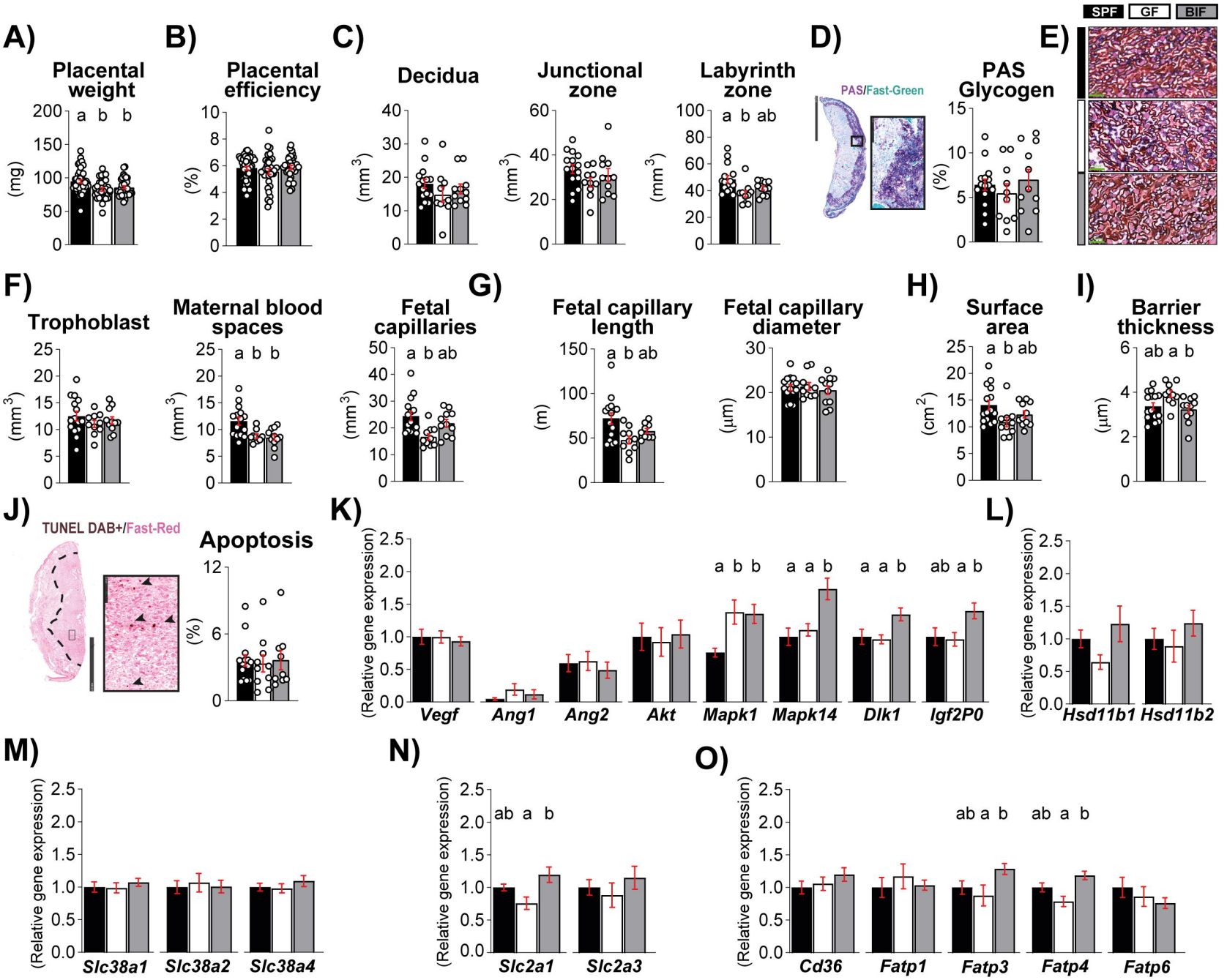
SPF
GF
BIF
A)
Placental weight
(mg)
a b b
B)
Placental efficiency
(%)
C)
Decidua
Junctional zone
Labyrinth zone
(mm3)
a b ab
D)
PAS/Fast-Green
PAS Glycogen
(%)
E)
F)
Trophoblast
Maternal blood spaces
Fetal capillaries
(mm3)
a b b
a b ab
G)
Fetal capillary length
(m)
Fetal capillary diameter
(µm)
H)
Surface area
(cm2)
I)
Barrier thickness
ab a b
J)
TUNEL DAB+/Fast-Red
Apoptosis
(%)
K)
(Relative gene expression)
a b b
a a b
a a b
ab a b
Vegf
Ang1
Ang2
Akt
Mapk1
Mapk14
Dlk1
Igf2P0
L)
Hsd11b1
Hsd11b2
M)
Slc38a1
Slc38a2
Slc38a4
N)
ab a b
Slc2a1
Slc2a3
O)
ab a b
ab a b
Cd36
Fatp1
Fatp3
Fatp4
Fatp6

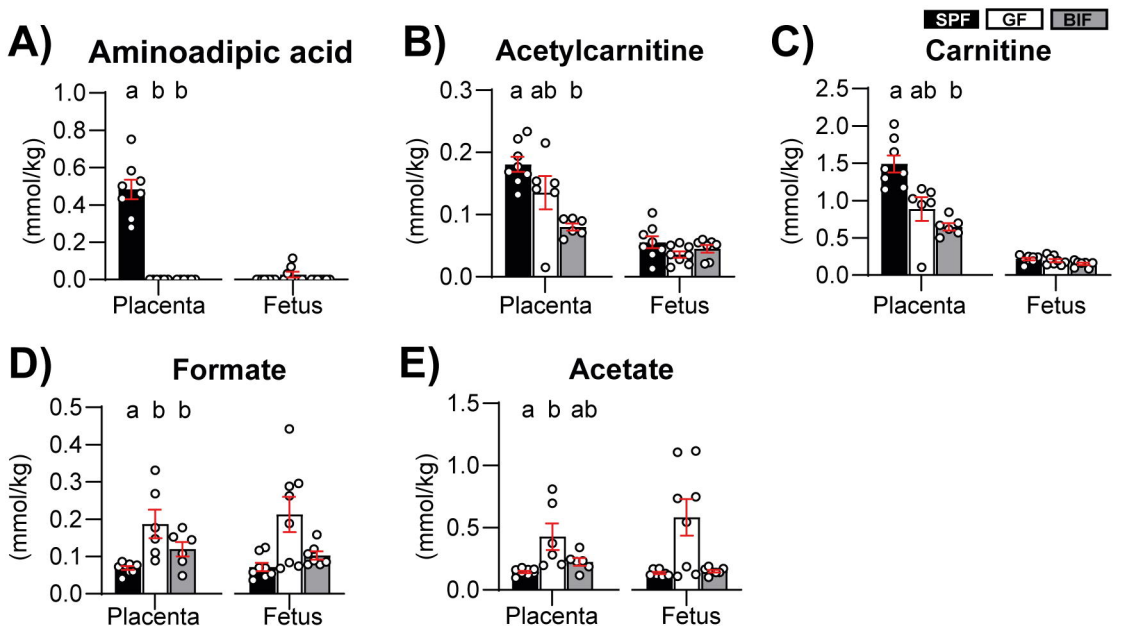
SPF
GF
BIF
A)
Aminoadipic acid
(mmol/kg)
1.0
0.8
0.6
0.4
0.2
0.0
a b b
Placenta
Fetus
B)
Acetylcarnitine
(mmol/kg)
0.3
0.2
0.1
0.0
a ab b
Placenta
Fetus
C)
Carnitine
(mmol/kg)
2.5
2.0
1.5
1.0
0.5
0.0
a ab b
Placenta
Fetus
D)
Formate
(mmol/kg)
0.5
0.4
0.3
0.2
0.1
0.0
a b b
Placenta
Fetus
E)
Acetate
(mmol/kg)
1.5
1.0
0.5
0.0
a b ab
Placenta
Fetus

Experimental groups

SPF

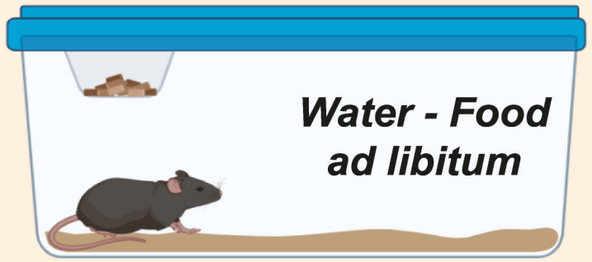

Individually Ventilated Cages

+

100 µL vehicle control solution

Vehicle control solution administrated on:
GD10 + GD12 + GD14

GF

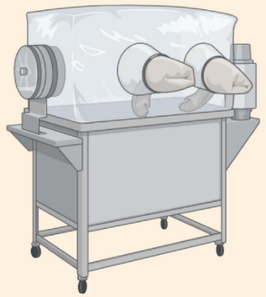

1) Germ free colony in flexible film isolator

Matings: Day of plug (GD0.5)
Housed in isolator: GD0 to GD9

Transfer to

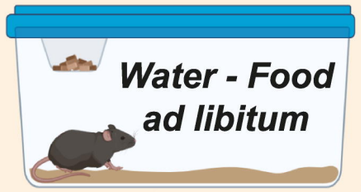

2) Individually Ventilated Cages

+

100 µL vehicle control solution

Vehicle control solution administrated on:
GD10 + GD12 + GD14

BIF

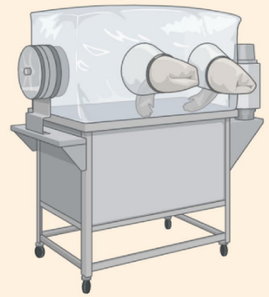

1) Germ free colony in flexible film isolator

Matings: Day of plug (GD0.5)
Housed in isolator: GD0 to GD9

Transfer to

2) Individually Ventilated Cages

+

100µL of B. breve UCC2003 at 10^{10} CFU/mL

B. breve UCC2003 administrated on:
GD10 + GD12 + GD14

Sampling

Maternal body composition and metabolism (GD16.5)	Fetal Biometry Placental structural/functional analysis (GD16.5)	Metabolomics: -Maternal caecum -Placental Lz -Fetal liver (GD16.5)	RNAseq of fetal liver (GD18.5)

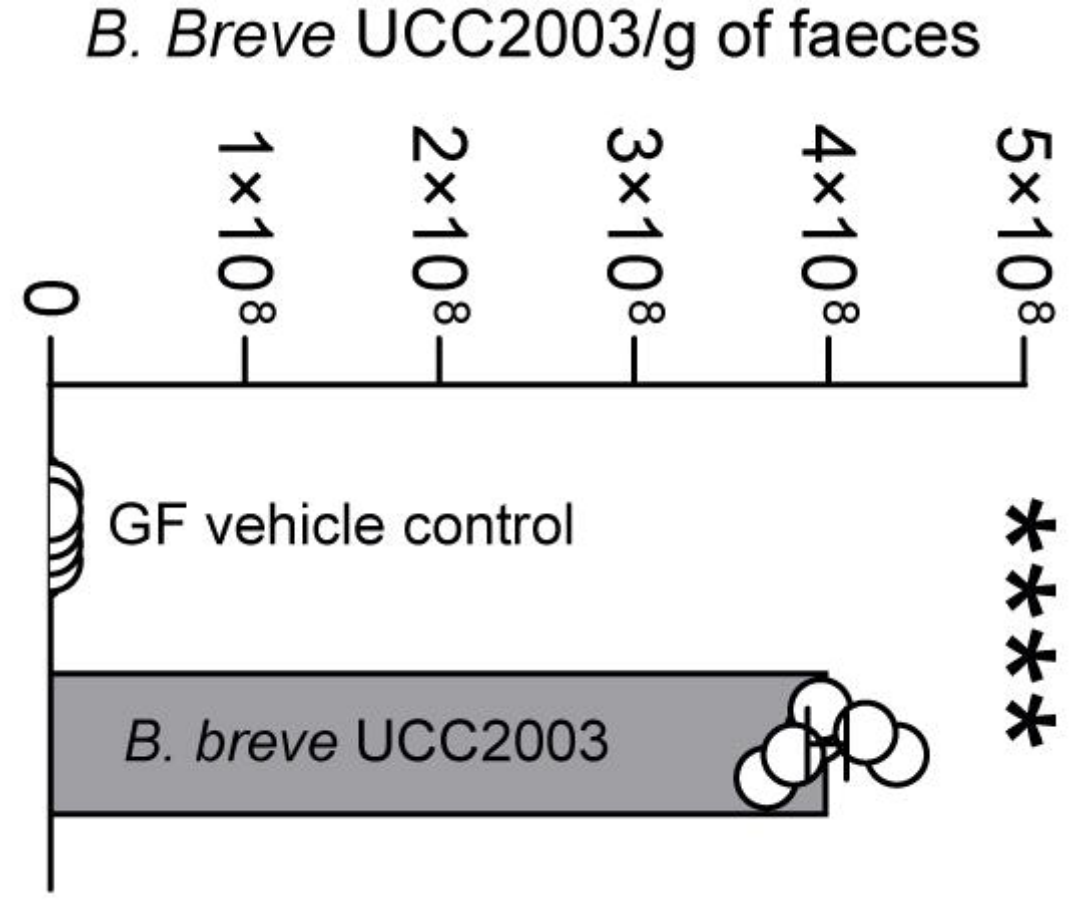
B. Breve UCC2003/g of faeces
0
1×10^8
2×10^8
3×10^8
4×10^8
5×10^8
GF vehicle control
B. breve UCC2003
*****

GF

BIF

Parameters compared to SPF and/or GF

Treatment with *B.breve*

Maternal body composition

Liver
Adipose
Spleen

ΔCaecum metabolites
methylbutyrate, butyrate, isobutyrate, propionate, aminopentanoate, citrulline, fucose, trimethylamine, malonate, methylamine, isovalerate, valerate, acetate

Acetate

↓weight & Lz volume
↓MBS & FC
↓SA
↑barrier thickness

↑Lz volume
↓FC
↑SA
↓barrier thickness

Igf2P0 *Dlk1* *Mapk14*

↑nutrient transporters

Slc2a1 *Fatp3-4*

Acetate
Acetylcarnitine
Carnitine

ΔPlacental metabolites
aminoadipic acid
formate
acetate

↑fetal loss
↓weight
↑SGA rate
↓liver size
↓glucose levels

↓fetal loss
↑weight
↓SGA rate
↑liver size
↑glucose levels

602 hepatic genes